Fixation of Powdered TiO₂ onto Metal Substrates by Electrophoretic Deposition and Its Use for Complete Decomposition of Volatile Organic Compounds

A. Maki, T. Ebara and Jin Mizuguchi

Graduate School of Engineering, Yokohama National University, Yokohama 240-8501, Japan

We are so far involved in complete decomposition of organic wastes as well as volatile organic compounds (VOC) by the use of thermally generated holes in TiO₂. In view of the practical use of the present system, fixation of TiO₂ powders onto a substrate seems to be the core technology. To realize this, we have tried in the present investigation to fix powdered TiO₂ onto SUS meshes or Ni-Cr wires by means of electrophoretic deposition. We have constructed two kinds of equipment. One is a cartridge system which includes ten pieces of the mesh disk coated with TiO₂ that are arranged vertically. The other is a "heater-built-in" system with a triple-coaxial structure equipped with Ni-Cr/Cr₂O₃/ TiO₂ wires. The former is used in combination with an external furnace; whereas the latter is a stand-alone system. Both systems exhibit excellent performance to completely decompose VOC into H₂O and CO₂. [doi:10.2320/matertrans.M2009074]

1. Introduction

Nowadays, emission of VOC (volatile organic compound) is a serious environmental problem, because VOC is directly responsible for air pollution, photochemical smog, sick house syndrome etc. Therefore, new technologies for the efficient removal of VOC are now in great demand, especially in printing and painting industries.

The purpose of the present paper is to introduce our novel application of semiconductors in a high-temperature region of about 350–500°C, quite in contrast to the conventional applications (transistor, laser, diode etc.) at room temperature. ZnO and TiO₂ were extensively investigated as photoconductors at the dawn of the electrophotography. Especially, TiO₂ has attracted as a photoconductor for direct digital color proofing system.[1] Nowadays, it has attracted attention as a material for photocatalyzers[2] and solar cells.[3,4]

We have previously shown, for the first time, that polycarbonate (PC) used as a material for optical discs can completely be decomposed in the presence of TiO₂ powders, releasing a huge amount of exothermic energy of about 1.85 kJ/g.[5] Since this moment, we have been conducting a series of investigations on the use of the present technology for complete decomposition of organic wastes (mainly thermoplastic and thermosetting polymers) as well as for removal of diesel exhaust.[6–12] Our system is characterized by the use of thermally excited holes at high temperatures (*e.g.*, about 350°C). Our system is similar to the photocatalyzer in the sense that powerful oxidative holes are utilized for decomposition of organic compounds. However, our system (*i.e.* thermal excitation) is much more advantageous in production number of holes to the photocatalyzer (*i.e.* optical excitation) by several orders of magnitude. The number of charge carriers by optical excitation is linearly proportional to the number of photons. However, the conductivity increase is normally limited at most 1–2 orders of magnitude, because the optical excitation occurs on the surface (where there are a number of recombination centers) and the charge carriers are mostly recombined immediately after excitation. On the other hand, thermal excitation creates charge carriers in the bulk as well as on the surface, and the number of charge
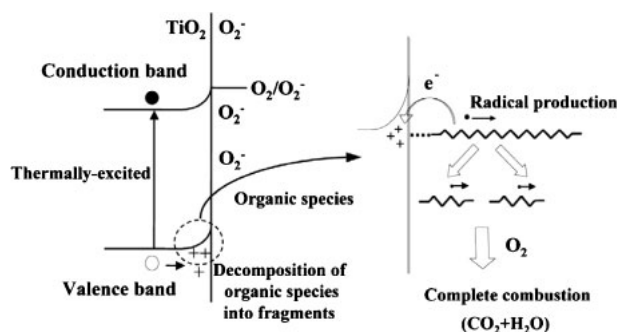

Fig. 1 Decomposition process of PC at the "TiO₂/PC" interface by means of thermally generated holes.

carriers increases exponentially as shown below. The number of charge carriers in semiconductors is determined by the product of the Fermi-Dirac distribution function and the density of states.[13] This gives an exponential function of $n = n_0 \exp[-E_g/2kT]$, where n denotes the number of carriers at a temperature of T, and E_g designates the band gap of a semiconductor. Simple calculation of the ratio of the carriers at room temperature (RT) and 350°C (*i.e.* n_{623K}/n_{RT}) in TiO₂ ($E_g = 3.2$ eV) gives a value of about 8.8×10^{13}. This number has approximately been confirmed in our experiment using single crystals of TiO₂ of the rutile phase.[7] That is, the resistivity of TiO₂ at RT was about 10^{11} Ω cm while only 15 Ω cm at 500°C, showing that a great number of charge carriers are formed by thermal excitation.

Figure 1 shows the decomposition process of polycarbonate (PC: used as the substrate for optical discs) into H₂O and CO₂ at 500°C in air. The initial step is the capture of bonded electrons from PC to form radicals by thermally generated holes, followed by their propagation throughout the polymer chain to break PC into fragments, leading to their complete combustion with oxygen to give only H₂O and CO₂.[7]

In our previous studies,[7–13] we worked with powdered TiO₂ in an autoclave based upon a fluidized bed system (Fig. 2). The present system features an extremely high collision frequency between VOC molecules and powdered TiO₂. However, the powder system is obviously not adequate for practical applications. For this reason, an attempt has
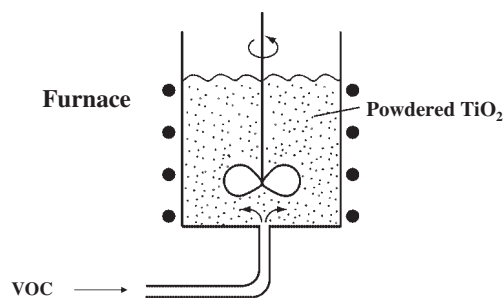
Fig. 2   Fluidized bed system with powdered TiO_2.

Fig. 4   Schematic representation of the SUS mesh before and after electrophoretic deposition of powdered TiO_2.

Fig. 3   Cartridge system with a lid which includes SUS meshes.

Fig. 5   Triple-coaxial system which has a dimension of 25 mm in diameter and 200 mm long.

been made in the present investigation to fix powdered TiO_2 onto SUS meshes, or Ni-Cr wires (*i.e.* heat element) by electrophoretic deposition. The electrophoretic deposition method[14] is a technology similar to electroplating and enables us to prepare catalyzer units of any shape with a simple and low-cost setup.

2.   Basic Design of Equipment for VOC Decomposition

We have fabricated two kinds of equipment. One is a cartridge system which includes mesh disks with TiO_2 that are arranged vertically as shown in Fig. 3. Figure 4 is a schematic drawing of the SUS mesh (diameter of the wire: $100\,\mu m$ and the spacing between wires: $250\,\mu m$) punched out from a sheet of the SUS mesh. Deposition of powdered TiO_2 is carried out onto the mesh, using the mesh as the electrode. The present devise is used in combination with an external furnace. The cartridge has a dimension of 25 mm in diameter and 70 mm long. Each mesh has a structure of SUS mesh/Cr_2O_3 (thickness: $1\,\mu m$)/TiO_2 (thickness: $3\,\mu m$). The present cartridge system is very similar in structure to the honeycomb system used widely in the field of catalyzers. Furthermore, this system is very flexible in widening or narrowing the spacing of the mesh wire, depending on the VOC flow rate. It is also possible to pile the mesh disk as many as possible.

The other equipment is a "heater-built-in" system using a Ni-Cr heating element (diameter: 0.5 mm). The equipment has a triple-coaxial structure. The core is a glass rod made of pyrex, together with two additional glass tubes, each of which was wound with a Ni-Cr/Cr_2O_3 (thickness: $1\,\mu m$)/TiO_2 (thickness: $3\,\mu m$) wire (Fig. 5). Here again, TiO_2 powders are directly fixed onto the heat element by electrophoretic
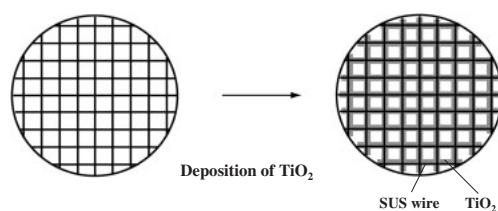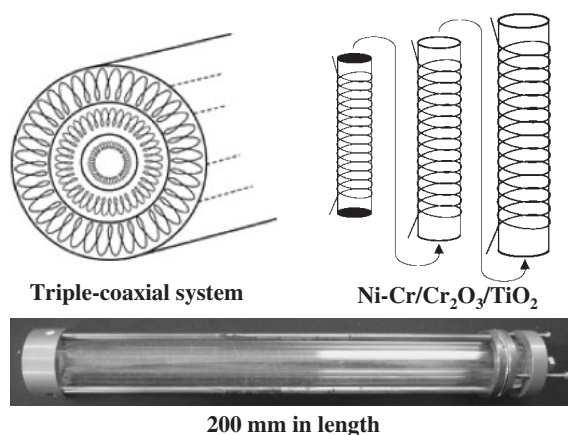
deposition. This is a stand-alone system, since the heat element is built-in.

3.   Experimental

3.1   Materials

Commercial TiO_2 powders of ST-01 were obtained from Ishihara Sangyo Kaisha, Ltd. This is of the anatase form with a specific surface of $298\,m^2/g$ (*ca.* 7 nm in average diameter). Tetramethylammonium hydroxide (TMAH: 15 wt% aqueous solution) was obtained from Wako Pure Chemical Industries, Ltd. Acetone of electronic grade and sulfuric acid of guaranteed grade were purchased from Junsei Chemical Co., Ltd. Nitrocellulose of RS-60 $[C_6H_7O_2(NO_2)(OH)]_n$ ($n = 360$) was obtained from KCNC Ltd. Ni-Cr wires (0.5 mm in diameter) and SUS304 meshes (wire diameter: $100\,\mu m$; spacing: $250\,\mu m$) were obtained from NILACO and Kyuho Kinzoku, respectively.

3.2   Preparation of the suspension

The typical composition of the suspension has been described in our previous report.[14] 10 g of ST-01 was suspended in 100 ml of an acetone solution containing 0.3 g of nitrocellulose. The suspension was conditioned in the presence of zirconia balls (0.2 mm in diameter) by a paint shaker for 30 min. Then, 50 ml of the suspension was placed into an electrolytic cell of 50 ml, and $12\,\mu l$ of TMAH and $4.0\,\mu l$ of sulfuric acid were added.

3.3   Preparation of a buffer layer

Electrophoretic deposition of powdered TiO_2 onto SUS mesh or Ni-Cr was quite successful. However, we often

found tiny cracks in the TiO$_2$ layer caused by thermal cycles between room temperature and 500°C. Since the crack is found to appear due to the difference in thermal expansion coefficient between metal and oxide, we have solved this problem by introducing a thin buffer layer of Cr$_2$O$_3$ between SUS mesh (or Ni-Cr) and TiO$_2$. A thin layer of Cr$_2$O$_3$ (about 1 μm) was prepared by oxidizing SUS meshes or Ni-Cr wires in wet hydrogen at 980°C for 1 h, using equipment as shown in Fig. 6. Under 980°C, H$_2$ cleans up the metal surface due to the reducing properties of H$_2$. Then, above 980°C, water decomposition takes place to oxidize the metal by means of released oxygen. This method provides us with a thin, solid layer of Cr$_2$O$_3$ (thickness: about 1 μm) of high quality.

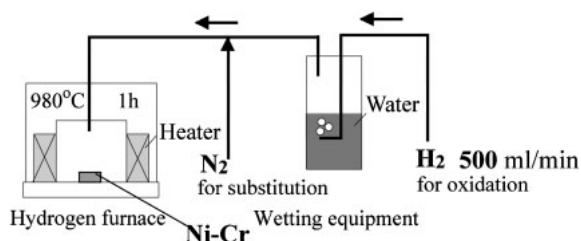Fig. 6 Equipment for oxidation of SUS meshes or Ni-Cr wires by wet hydrogen.

3.4 Equipment for electrophoretic deposition of powdered TiO$_2$

Figure 7 illustrates schematically the experimental setup for the electrophoretic deposition. A SUS mesh or Ni-Cr wire with a buffer layer of Cr$_2$O$_3$ was used as the anode while an Al cylinder was served as the counter electrode.

3.5 Equipment

Scanning electron microscope (SEM) pictures were taken with a VE-8800 SEM equipment from KEYENCE. Raman spectra were measured by an NRS-3100 laser Raman spectrophotometer from JASCO. Specific surface was measured by a Monosorb (LOOP) MS-22 from YUASA IONICS Inc. The decomposed gas was analyzed as a function of temperature by means of a RG-102 quadrupole-massfilter (ULVAC).

3.6 Experiment for VOC decomposition

Figures 8(a) and 8(b) show the schematic representation of the equipment for VOC decomposition for the cartridge and the triple-coaxial systems. Toluene was used as a representative VOC for decomposition experiment. The toluene concentration was about 1 vol% and the air was used as the carrier gas whose flow rate was 100 ml/min for the cartridge system and 50 ml/min for the triple-coaxial system. The decomposed gas was analyzed by Q-mass.
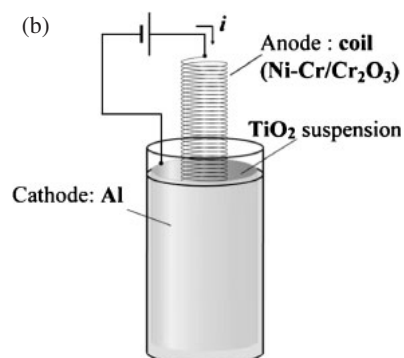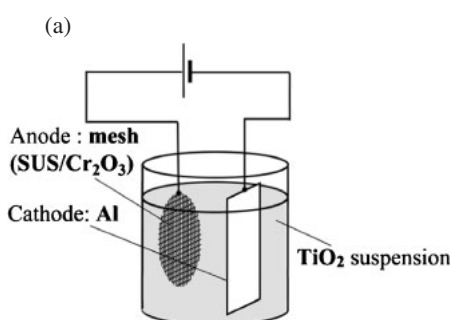

Fig. 7 Schematic illustration of the electrophoretic deposition: (a) for SUS meshes and (b) for Ni-Cr spirals.

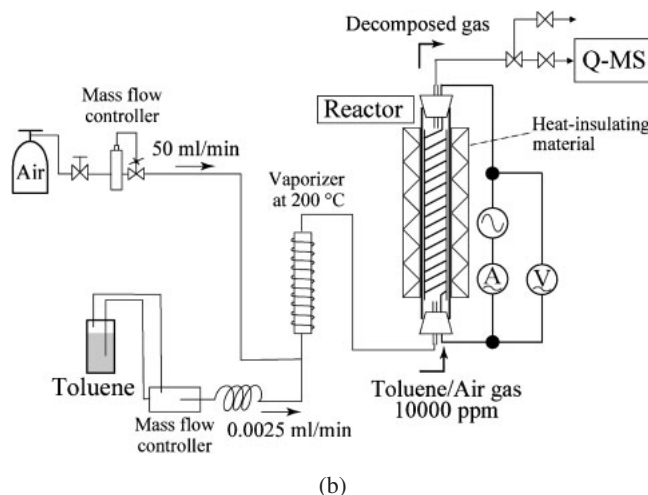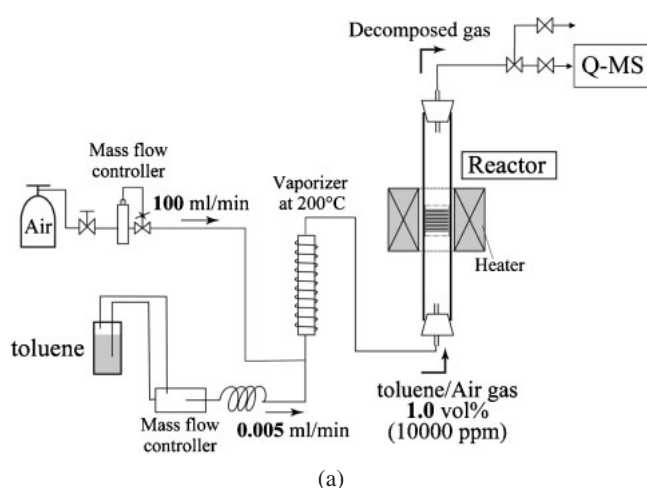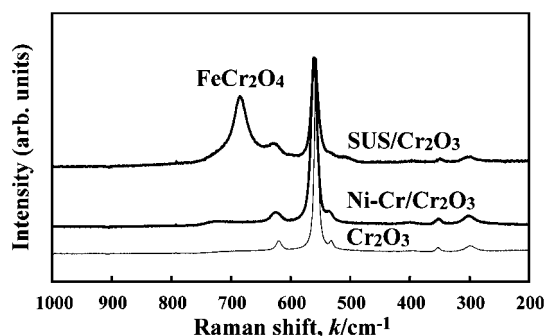Fig. 8 Schematic representation of the equipment for VOC decomposition: (a) for the cartridge system and (b) for the triple-coaxial system.

Fig. 9 Raman spectra of SUS/Cr_2O_3, Ni-Cr/Cr_2O_3, and commercially available powdered Cr_2O_3.

4. Results and Discussion

4.1 Identification of the Cr_2O_3 layer

Figure 9 shows the Raman spectra of the oxide layers prepared on SUS meshes or Ni-Cr wires by wet hydrogen, together with commercially available powdered Cr_2O_3. The spectrum of the oxide on Ni-Cr is in good accord with that of powdered Cr_2O_3 (300, 352, 535, 560, and 625 cm^{-1}), while one additional band appears around 700 cm^{-1} in the spectrum of the oxide on SUS meshes which is presumably due to the $FeCr_2O_4$.[15]

Figures 10(a) and 10(b) show the SEM pictures of SUS/Cr_2O_3 prepared by wet hydrogen, taken with different magnifications. The surface looks very even and smooth.

4.2 Characteristics of the electrophoretic deposition

Figure 11 shows the amount of deposit *vs.* deposition time as a function of applied voltage, where the amount of deposit (mg/cm^2) was calculated from the amount of deposit on the electrode together with the surface area of the electrode. The thickness of the deposited layer is also shown on the right vertical axis. The amount of deposit increases with time and applied voltage. Our target thickness of the deposit layer is about 3–5 μm. So the optimum condition for deposition is: 100 V for 0.01 s.

Figures 12(a) and 12(b) show the SEM pictures of electrophoretically deposited TiO_2-layer on a SUS/Cr_2O_3 mesh, taken with different magnifications. The sample of SUS/Cr_2O_3/TiO_2 was heat-cycled ten times between room temperature and 500°C. Neither cracks nor peeling-off of the TiO_2 layer was observed, indicating that the buffer layer is effective in suppressing the cracks and peeling-off.

4.3 Surface area of wire samples

Table 1 shows the surface area of Ni-Cr, Ni-Cr/Cr_2O_3, and Ni-Cr/Cr_2O_3/TiO_2 wires (unit: m^2/cm). The values normalized by that of Ni-Cr are shown on the right column. The surface area of Cr_2O_3 is larger than of Ni-Cr by 13%. The surface area of TiO_2 is one order of magnitude larger than that of Ni-Cr. This indicates that the large specific surface of original TiO_2-powders is well preserved even in electrophoretically deposited layers.

4.4 VOC Decomposition experiment with the cartridge system or the triple-coaxial system

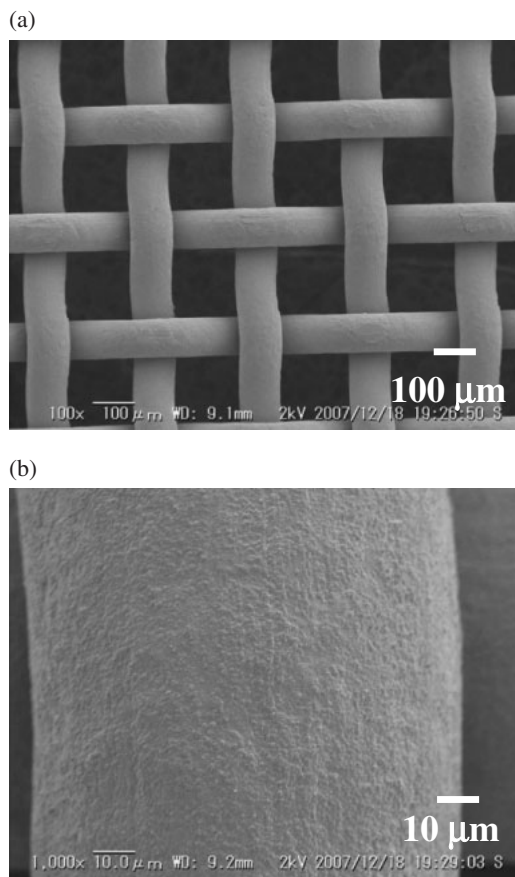Decomposition experiment of toluene was carried out,

(a)

(b)

Fig. 10 SEM pictures of the SUS/Cr_2O_3 prepared by wet hydrogen, taken with different magnifications.
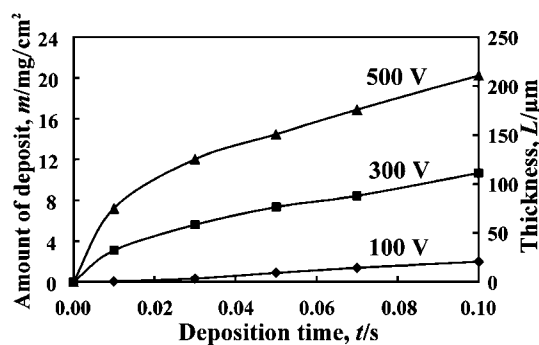

Fig. 11 Characteristics of the electrophoretic deposition of powdered TiO_2 as a function of deposition time and applied voltage. The optimum condition for the preparation of a deposit layer of about 3–5 μm is: 100 V for 0.01 s.

using a cartridge which includes ten pieces of the mesh disk with TiO_2 (Fig. 3: SUS mesh/Cr_2O_3/TiO_2). Figure 13(a) shows the decomposition of toluene as a function of temperature. Toluene starts to decompose around 350°C and is nearly completed (about 95%) at 500°C, accompanied by consumption of oxygen and also by production of H_2O and CO_2. No other species were detected in decomposed gases except for N_2 and O_2 in air. This result indicates that toluene is completely decomposed into H_2O and CO_2.

Figure 13(b) shows the decomposition of toluene in the triple-coaxial system (Fig. 5: Ni-Cr/Cr_2O_3/TiO_2) as a function of power consumption, or of temperature. Toluene decomposition starts around 230°C and is nearly completed at
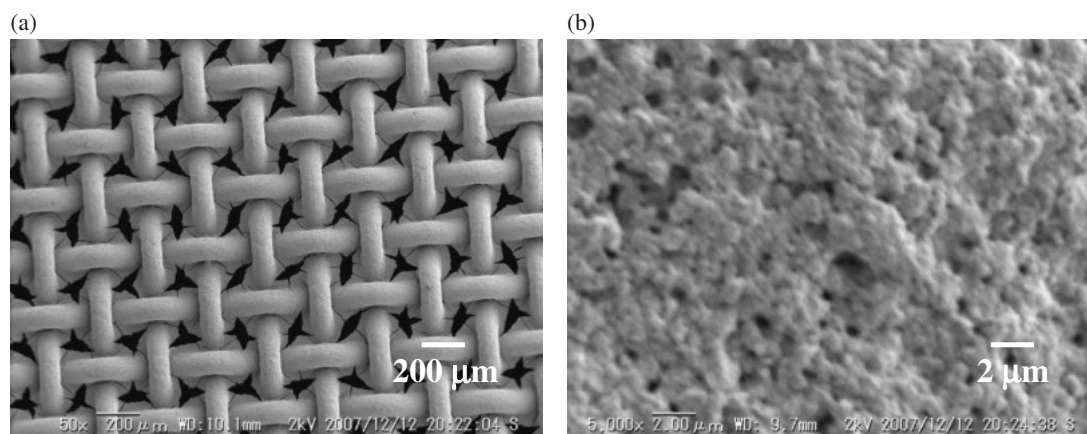
(a)

(b)

Fig. 12 SEM pictures of electrophoretically deposited TiO₂ on SUS/Cr₂O₃, taken with different magnifications.

Table 1 Surface area of Ni-Cr, Ni-Cr/Cr₂O₃, and Ni-Cr/Cr₂O₃/TiO₂.

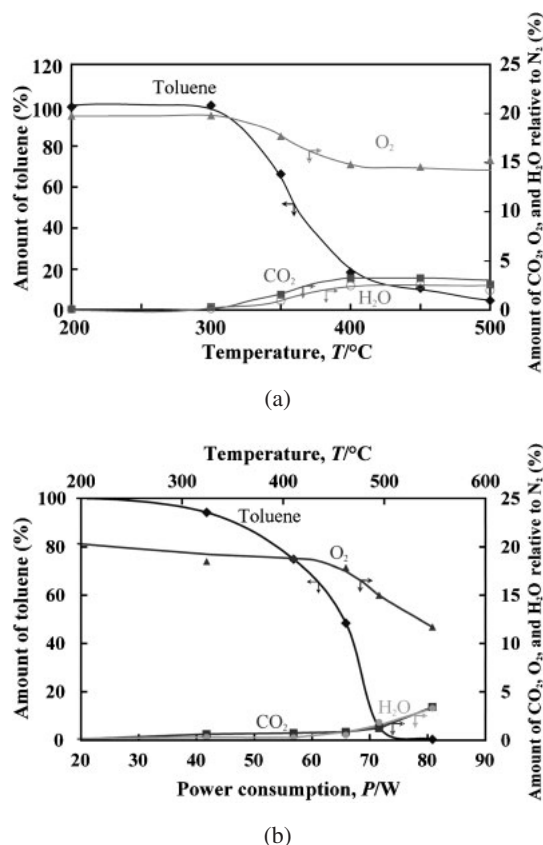|	Surface area, $L^2/m^2/cm$	Normalized value by that of Ni-Cr
Ni-Cr	2.66×10^{-4}	1.00
Ni-Cr/Cr₂O₃	3.01×10^{-4}	1.13
Ni-Cr/Cr₂O₃ with TiO₂	2.60×10^{-3}	9.77

(a)

(b)

Fig. 13 Decomposition of toluene in air: (a) with a cartridge system composed of ten pieces of the SUS mesh and (b) with a triple-coaxial system.

about 525°C. The power consumption at this point amounts to about 75 W. The decomposition of toluene is accompanied by the decrease of O₂ and increase of CO₂ and H₂O. No additional fragments of toluene could be observed in the mass spectra during the decomposition process. The present experiment suggests that our "heater-built-in" system (Ni-Cr/Cr₂O₃/TiO₂) basically works well and can be a compact, high-performance system with low cost in the future.

5. Conclusions

Novel systems composed of SUS mesh disks (SUS/Cr₂O₃/TiO₂) or "heater-built-in" triple-coaxial system (Ni-Cr/Cr₂O₃/TiO₂) have been developed for the removal of VOC. The present cartridge system has a honeycomb-like structure and is used in combination with an external system. On the other hand, the triple-coaxial system is a "heater-built-in" stand-alone system. Both of these exhibit excellent performance for the removal of VOC.

REFERENCES

1) Y. Ishibai, M. Okada, H. Murakami, S. Murasawa, M. Yoshiyama, T. Ide and T. Kawanabe: Proc. SPIE Vol. 1670, Color Hard Copy Graphic Arts, (The International Society for Optical Engineering 1992) pp. 287–294.
2) R. Wang, K. Hashimoto, A. Fujishima, M. Chikuni, E. Kojima, A. Kitamura, M. Shimohigoshi and T. Watanabe: Nature **388** (1997) 431–432.
3) M. Zukalová, A. Zukal, L. Kavan, M. K. Nazeeruddin, P. Liska and M. Grätzel: Nano Lett. **5** (2005) 1789–1792.
4) T. Miyasaka, Y. Kijitori and M. Ikegami: Electrochem. **75** (2007) 2–12.
5) J. Mizuguchi: J. Electrochem. Soc. **148** (2001) J55–J58.
6) J. Mizuguchi and T. Shinbara: J. Appl. Phys. **96** (2004) 3514–3519.
7) T. Shinbara, T. Makino, K. Matsumoto and J. Mizuguchi: J. Appl. Phys. **98** (2005) 044909 1–5.
8) T. Makino, K. Matsumoto, T. Ebara, T. Mine, T. Ohtsuka and J. Mizuguchi: Jpn. J. Appl. Phys. **46** (2007) 6037.
9) K. Matsumoto, T. Makino, T. Ebara and J. Mizuguchi: J. Chem. Eng. Jpn. **41** (2008) 51–56.
10) K. Matsumoto, Y. Sato, T. Ebara and J. Mizuguchi: J. Chem. Eng. Jpn. **41** (2008) 57–61.
11) D. Yamaguchi, S. Suzuki and J. Mizuguchi: J. Chem. Eng. Jpn. **41** (2008) 929–932.
12) D. Yamaguchi, S. Suzuki and J. Mizuguchi: Mater. Trans. **50** (2009) 415–418.
13) C. Kittel: *Introduction to Solid State Physics* (8th Edition), (John Wiley & Sons, New York, U. S. A., 2005).
14) J. Mizuguchi, K. Sumi and T. Muchi: J. Electrochem. Soc. **130** (1983) 1819–1825.
15) N. Birks and G. H. Meier: *Introduction to the High Temperature Oxidation of Metals*, (Edward Arnold, London, 1983).